

Comprehensive Analysis of Selenium Metabolism and Selenoproteins-Associated Gene Signatures in Ulcerative Colitis

Chang Gao^{1,*}, Jiaojiao Wang^{1,*}, Siqi Dai², Danning Wang¹, Jianwei Wang^{1,2}

¹Department of Oncology, The Fourth Affiliated Hospital of School of Medicine, and International Institutes of Medicine, Zhejiang University School of Medicine, Yiwu, 322000, People's Republic of China; ²Department of Colorectal Surgery and Oncology, Key Laboratory of Cancer Prevention and Intervention, Ministry of Education, Second Affiliated Hospital, Zhejiang University School of Medicine, Hangzhou, 310009, People's Republic of China

*These authors contributed equally to this work

Correspondence: Jianwei Wang, Email sypzju@zju.edu.cn

Background: Ulcerative colitis (UC) is a chronic inflammatory bowel disease marked by persistent mucosal inflammation. Oxidative stress plays a vital role in UC pathogenesis. Selenium (Se), an essential trace element, functions via selenoproteins and metabolites. Selenocysteine (Sec), the 21st amino acid, is incorporated into selenoproteins with strong antioxidant and anti-inflammatory properties. However, the role of selenium metabolism and selenoproteins (SeMet) in UC remains poorly understood.

Methods: Gene expression and clinical data from UC patients and healthy controls were obtained from the GEO database. SeMet-related gene sets were collected from Molecular Signatures Database (MSigDB). Weighted gene co-expression network analysis (WGCNA) and differential expression analysis identified key modules and genes associated with UC. Machine learning algorithms were used to screen signature genes and construct a UC risk prediction model. Single-cell RNA sequencing (scRNA-seq) was performed to examine gene expression at the cellular level. Expression of differentially regulated genes (DRGs) and signature genes was validated using quantitative polymerase chain reaction (qPCR), Western blotting, and immunohistochemistry (IHC).

Results: DRGs were significantly upregulated in UC and used to classify 161 UC samples into two subtypes. Six candidate signature genes were identified by integrating WGCNA and machine learning, showing high diagnostic potential and inter-correlation. scRNA-seq revealed upregulation of many selenoproteins in epithelial cells and downregulation of SELENOP in immune cells. The six signature genes were consistently upregulated across multiple cell types. WARS1 (tryptophanyl-tRNA synthetase 1), one of the signature genes, responded strongly to oxidative stress, and its knockdown elevated inflammatory cytokine levels.

Conclusion: SeMet-related genes are crucial in UC pathogenesis, particularly through antioxidant defense and immune modulation. The identified six-gene signature offers promising diagnostic and therapeutic potential for UC.

Keywords: ulcerative colitis, selenium metabolism, selenoproteins, oxidative stress, WARS1

Introduction

UC is a chronic, idiopathic inflammatory bowel disease (IBD) characterized by persistent mucosal inflammation. It affects millions of individuals worldwide, with its prevalence steadily increasing in recent years.¹ The development of UC is multifactorial, involving genetic susceptibility, impaired epithelial barrier integrity, dysregulated immune responses, and environmental triggers.² Among these factors, the essential trace element Se has attracted growing attention due to its antioxidant³ and anti-inflammatory properties, as well as its potential therapeutic value in UC.^{4,5}

Selenium exerts its biological effects primarily through selenoproteins—proteins that incorporate the amino acid Sec.⁶ The human genome encodes 25 selenoproteins,⁷ many of which, such as glutathione peroxidases (GPx), thioredoxin reductases (TrxR), and iodothyronine deiodinases (DIO), serve as intracellular antioxidants with well-established oxidoreductase functions.⁸ Recent studies have shown that selenoproteins play a critical role in the onset and progression

of UC. In knockout mouse models, both GPx-1 and GPx-2 have demonstrated protective roles against intestinal inflammation; their simultaneous deletion results in ileocolitis.⁹ Although GPx-3 deletion alone does not induce colitis, it significantly exacerbates disease severity in dextran sulfate sodium (DSS)-treated GPx-3^{-/-} mice.¹⁰ Additionally, Selenoprotein S (SELENOS) expression increases in vivo alongside the endoplasmic reticulum (ER) stress marker GRP78 following DSS treatment.¹¹ In patients with UC, Selenoprotein P (SELENOP) is downregulated in colon biopsy samples, with its expression inversely correlated with disease severity as measured by endoscopy.¹² Specific deletion of Selenoprotein I (SELENOI) in intestinal epithelial cells triggers ferroptosis, impairs intestinal regeneration, and reduces colonic tumor growth.¹³ Furthermore, Selenoprotein W (SELENOW) is essential for resolving experimental colitis by regulating the epidermal growth factor receptor (EGFR) and Yes-associated protein 1 (YAP1) signaling pathways.¹⁴

In this study, we investigated the role of SeMet-related genes in UC using integrative bioinformatics and experimental approaches. Gene expression and clinical data were obtained from the GEO database, and SeMet-related gene sets were collected from MSigDB. WGCNA and differential expression analysis were performed to identify key modules and DRGs. Based on eleven upregulated SeMet-related genes, 161 UC patients were stratified into two molecular subtypes. Machine learning algorithms were applied to identify six candidate signature genes with high diagnostic potential, which were then used to construct a UC risk prediction model. Single-sample gene set enrichment analysis (ssGSEA) revealed strong correlations between signature genes and immune cell infiltration. ScRNA-seq analysis showed upregulation of several selenoproteins in epithelial cells and downregulation of SELENOP in immune cells. We further validated the elevated expression of selenoprotein M (SELENOM) and selenoprotein N (SELENON) in UC tissues and demonstrated that WARS1 responds to oxidative stress, with its knockdown increasing inflammatory cytokine levels. These findings enhance our understanding of SeMet-related genes in UC and highlight their diagnostic and therapeutic relevance.

Materials and Methods

Sources and Processing of Datasets

Eight UC datasets were obtained from the Gene Expression Omnibus (GEO, <https://www.ncbi.nlm.nih.gov/geo/>) database, including GSE75214,¹⁵ GSE87466,¹⁶ GSE47908,¹⁷ GSE206171, GSE48958,¹⁸ GSE9452,¹⁹ GSE38713,²⁰ and GSE13367.²¹ Next, the GSE75214 and GSE87473 datasets were combined, and batch effects in the gene expression data were addressed using the “comBat” function from the “sva” package in R. The datasets GSE47908, GSE206171, and GSE48958 were used as test sets for machine learning. The gene set “Selenium Metabolism and Selenoproteins” was obtained from the Molecular Signatures Database v5.0 (<http://software.broadinstitute.org/gsea/msigdb/index.jsp>).

Immune Cell Infiltration Analysis

ssGSEA²² was employed to estimate the relative infiltration levels of immune cell types in the UC microenvironment. Gene sets specific to various immune cell types were obtained from the study by Charoentong et al.²³ The analysis was conducted using the R package GSVA, which calculates enrichment scores for individual gene sets across samples based on transcriptome data.

Defining SeMet-Associated Molecular Subtypes in Ulcerative Colitis

Unsupervised hierarchical clustering analysis was then conducted on 161 UC samples using the “ConsensusClusterPlus” R package, based on the significantly upregulated DRGs.²⁴ Molecular pathways with significant enrichment were identified based on gene set variation analysis (GSVA) scores across distinct subtypes. Immune cell infiltration variations between these subtypes were then analyzed.

Gene Co-Expression Network Construction

To identify co-expressed gene modules and investigate their relationships with various traits or phenotypes, we employed WGCNA analysis.^{25,26} Initially, the necessity for filtering gene samples was assessed using the “goodSamplesGenes” function from the “WGCNA” package (v1.69). Next, we constructed an adjacency matrix by calculating Pearson’s correlation coefficients between all gene pairs. This matrix was then used to build a scale-free co-expression network,

applying a soft-thresholding technique that amplifies strong gene correlations and suppresses weaker ones. Finally, the adjacency matrix was transformed into a topological overlap matrix (TOM), which quantitatively reflects the similarity between node pairs based on their weighted correlations.

Identification of Feature Genes and Construction of a Risk Model Based on Machine Learning Algorithms

In order to identify key genes with potential diagnostic value, we applied two advanced feature selection methods: the Least Absolute Shrinkage and Selection Operator (LASSO) and Support Vector Machine-Recursive Feature Elimination (SVM-RFE). Genes identified by both algorithms were considered as potential candidates for further investigation. Following this, we developed a UC risk prediction model by integrating 15 different machine learning algorithms and evaluating 207 distinct combinations of these models. The algorithms incorporated included: neural networks, logistic regression, linear and quadratic discriminant analysis, K-nearest neighbors (KNN), decision trees, random forests, XGBoost, ridge regression, LASSO regression, elastic net regression, support vector machines, gradient boosting machines, stepwise logistic regression, and naive Bayes.^{27,28}

Gene Set Enrichment Analysis (GSEA) and Correlation Analysis

To explore the functional relevance of specific genes in the context of UC, we analyzed their expression profiles in relation to other mRNAs through Pearson correlation using transcriptomic datasets from the GEO database. To gain insights into the potential biological pathways involved, Gene Set Enrichment Analysis (GSEA) was carried out utilizing the R package “clusterProfiler”.²⁹ For this study, the “c2.cp.kegg.v7.5.1.entrez.gmt” collection was used in GSEA.

Single-Cell Analysis

To further investigate the signature genes and DRGs at the single-cell level in UC, the GSE214695³⁰ and GSE231993³¹ datasets were downloaded from the GEO database for single-cell sequencing analysis. High-throughput sequencing data were analyzed using the “Seurat” package in R to construct single-cell expression profiles. To reduce dimensionality and identify clusters based on highly variable genes, principal component analysis (PCA) was initially performed. For further nonlinear dimensionality reduction and visualization, the UMAP algorithm was applied. To correct for batch effects between control and UC samples, the “Harmony” R package was utilized. Cell type annotation was performed using the “SingleR” R package in combination with manual curation based on published literature, ensuring both computational accuracy and biological relevance. Marker genes for each cell population were identified using the FindAllMarkers function. The expression patterns and distribution of both signature genes and DRGs were examined across individual cell clusters. To explore intercellular communication patterns within the UC microenvironment, the “CellChat” R package was employed. Finally, the Monocle2 package was employed to perform pseudotime analysis on macrophages.

Cell Culture

The HCT116 human colon cancer cell line and NCM460 normal human colonic epithelial cell line were obtained from the American Type Culture Collection. The cells were cultured in complete DMEM medium (Thermo Scientific, Waltham), supplemented with 10% fetal bovine serum (FBS, Gibco, Thermo Scientific, Waltham), in a CO₂ incubator set at 5% CO₂ and 37°C.

Western Blotting

The cells were lysed with ice-cold RIPA lysis buffer (Servicebio, China) containing protease inhibitors and then centrifuged at 4°C (12,000 rpm for 20 min). The protein supernatant was then quantified using a BCA protein assay kit (Biyuntian, China). After protein denaturation, 30 µg of protein were separated on 10% gels by SDS-PAGE and transferred to a PVDF membrane (Millipore, USA). After blocking with 5% skim milk in TBS-T, the membrane was incubated overnight at 4°C with the following antibodies: anti-SELENOM (SANTA, 1:400); anti-SELENON (SANTA,

1:400); anti-GPX1/2 (SANTA, 1:400); anti-WARS1 (Proteintech, 1:1000); anti-GAPDH (Proteintech, 60004-1-Ig). The membranes were then incubated with goat anti-rabbit (Proteintech, RGAR001, 1:5000) or mouse IgG secondary antibodies (Proteintech, RGAM001, 1:5000) for 1 hour. The membranes were then washed with TBS-T three times (5 min per wash) and finally visualized using enhanced chemiluminescence substrate.

RNA Transcription and Real-Time PCR

Total RNA was extracted from tissue and cell samples of UC using the RNAiso kit (Vazyme RC201). mRNA was then reverse transcribed into complementary DNA (cDNA) using the cDNA synthesis kit (Vazyme R222-01). RT-qPCR was subsequently performed using the SYBR Green Master Mix reagent (Vazyme Q131). Relative expression levels were determined using the $2^{-\Delta\Delta C_t}$ method, with GAPDH used as an internal control.

Histology and Immunohistochemistry

Colon tissue samples were preserved in 4% paraformaldehyde, embedded in paraffin, and sectioned into 5 μm slices for histological analysis. For immunofluorescence staining, antigen retrieval was performed by heating the sections in a sodium citrate buffer solution. To suppress endogenous peroxidase activity, tissue slices were treated with 3% hydrogen peroxide. Subsequently, non-specific binding sites were blocked using 3% bovine serum albumin (BSA) for 30 minutes at ambient temperature. Primary antibodies were applied and incubated overnight at 4 °C. The next day, after applying the corresponding secondary antibodies, the sections were developed with DAB, counterstained with hematoxylin, and examined under a standard brightfield microscope.

Animals and Animal Models

All animal experiments in this study were conducted in accordance with the welfare and ethical guidelines for experimental animals established by Zhejiang University and approved by the Animal Experimental Ethics Committee. Wild-type C57BL/6 mice (6 weeks old) were acquired from GemPharmatech (Jiangsu, China) and maintained in a specific-pathogen-free (SPF) animal facility. The mouse colitis model was induced by administering 3% dextran sulfate sodium (DSS, Yeasen Biotech, Shanghai, China) dissolved in filter-purified and sterilized water ad libitum to the Wild-type C57BL/6 mice for 7 days.

Sample Collection

Five patients diagnosed with UC and five healthy controls (HC) were recruited from the Fourth Affiliated Hospital of Zhejiang University. Intestinal mucosal biopsies were obtained during endoscopic examination. All participants provided written informed consent prior to anesthesia. The study was approved by the Medical Ethics Committee of the Fourth Affiliated Hospital of Zhejiang University and conducted in accordance with the Declaration of Helsinki.

Results

Variations of SeMet-Related Genes in Active Ulcerative Colitis

To investigate alterations in SeMet-related genes associated with active UC, datasets GSE75214 and GSE87466 were merged, and batch effects were removed. Differentially regulated genes (DRGs) were then identified using the “limma” package in R. As shown in [Figure 1A](#), 27 DRGs displayed distinct expression patterns between UC and healthy controls. Specifically, genes such as FOS, SELENOM, SELENON, DIO2, GPX1, GPX2, SELENOK, RELA, SELENOS, CREM, and TRNAU1AP were significantly upregulated, while SELENBP1, SELENOW, GPX4, TXNRD2, and others were notably downregulated. Genes with $|\log_2FC| > 0.5$ and adjusted P-value < 0.05 were selected for downstream analysis. [Figure 1B](#) presents the correlation matrix among the 11 most significantly dysregulated DRGs. To explore immune dysregulation in UC and the involvement of DRGs, we applied ssGSEA to quantify the relative abundance of various immune cell types in both UC and control samples. As shown in [Figure 1C](#), immune cell populations such as activated dendritic cells, CD8⁺ T cells, B cells, natural killer (NK) cells, macrophages, and neutrophils were significantly enriched in UC tissues. Correlation analysis between DRGs and immune infiltration revealed distinct association patterns

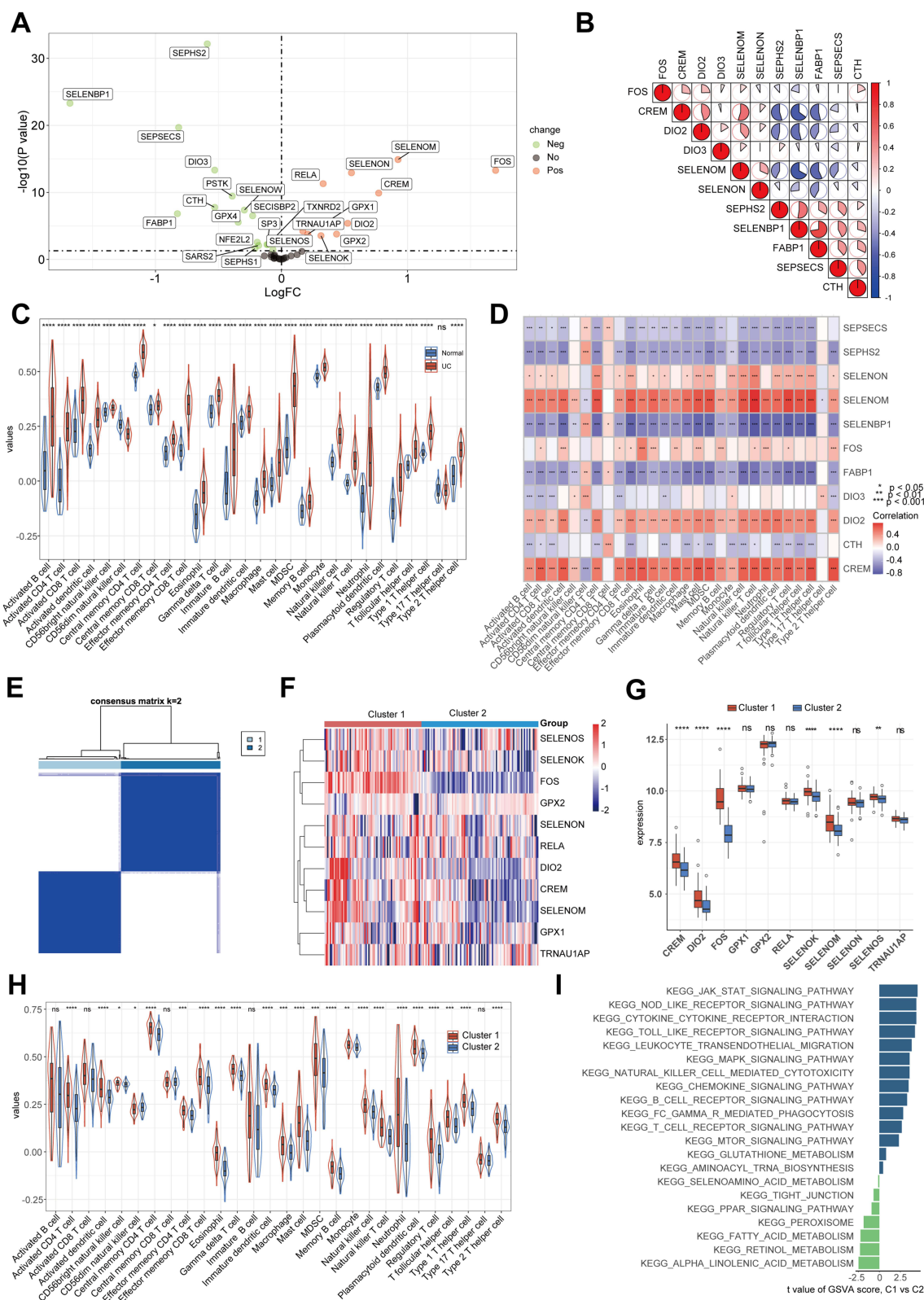


Figure 1 Variations of SeMet-Related Genes in Active Ulcerative Colitis. **(A)** Scatter plots showing differential expression of SeMet-related genes between UC and control groups. **(B)** Pie chart size reflects correlation coefficients among genes. **(C)** Violin plots comparing immune cell infiltration between UC and controls. **(D)** Correlation analysis of 11 differentially expressed DRGs and immune cell types. **(E)** Consensus clustering heatmap for $k = 2$. **(F)** Heatmap of differential expression of 11 DRGs across identified subtypes. **(G)** Boxplots displaying subtype-specific expression of 11 DRGs. **(H)** Violin plots illustrating immune cell infiltration differences between subtypes. **(I)** GSEA results comparing pathway enrichment between cluster 1 and cluster 2. Statistical significance is indicated as follows: ns, not significant; * $P < 0.05$; ** $P < 0.01$; *** $P < 0.001$; **** $P < 0.0001$.

(Figure 1D). SELENOM and SELENON were positively correlated with central memory CD4⁺ T cells, effector memory CD8⁺ T cells, and NK cells, whereas SEPSECS, SEPHS2, and SELENBP1 showed inverse correlations with neutrophils and macrophages. These findings suggest that DRGs may influence disease progression in UC through modulation of immune cell infiltration and activity.

Consensus clustering analysis of 161 active UC samples was performed based on the expression profiles of eleven upregulated DRGs. The optimal number of clusters was determined to be $k = 2$, supported by multiple evaluation metrics, including the structure of the consensus matrix (Figure 1E), the shape of the cumulative distribution function (CDF) curve (Figure S1A), and the inflection point in the CDF area change plot (Figure S1B). Consequently, two molecular subtypes associated with selenoproteins and selenium metabolism were identified and designated as Cluster 1 ($n = 73$) and Cluster 2 ($n = 88$). The heatmap and boxplot (Figure 1F and G) revealed significantly higher expression levels of SELENOK, SELENOM, SELENOS, CREM, and DIO2 in Cluster 1 compared to Cluster 2. Immune profiling demonstrated that activated CD4⁺ T cells, activated dendritic cells, effector memory CD8⁺ T cells, neutrophils, and macrophages were significantly enriched in Cluster 1 relative to Cluster 2 (Figure 1H). Gene set variation analysis (GSVA) further indicated that Cluster 1 was positively enriched in multiple immune-related pathways, including natural killer cell-mediated cytotoxicity, JAK-STAT signaling, toll-like receptor signaling, and NOD-like receptor signaling, whereas it was negatively enriched in selenocysteine metabolism and the PPAR signaling pathway (Figure 1I). These findings suggest that patients in Cluster 1 are likely in a stage characterized by pronounced inflammatory responses and impaired selenoprotein function. Given the classification of selenoproteins into housekeeping and stress-related types,³² we performed differential expression analysis comparing selenoprotein expression between inactive and active colitis patients using the GSE75214 dataset. This analysis identified significant upregulation of SELENOM, SELENOS, and DIO2 in active colitis (Figure S1C), supporting their involvement during periods of inflammatory activity.

Verification of Signature Genes and Construction of a Prediction Model

To identify genes strongly associated with clinical traits, we selected the top 25% of genes showing the highest variability between UC and healthy control samples for WGCNA. Outlier samples were removed, and a soft-thresholding power of $\beta = 18$ was selected based on the scale-free topology criterion (cutoff = 0.8; Figure S1D). Using the dynamic tree cut algorithm, nine distinct gene modules were identified, each represented by a unique color. Correlation analysis between module eigengenes and clinical traits revealed that the pink module (containing 202 genes) exhibited the strongest association with UC status (Figures 2A and S1E). A separate WGCNA was conducted based on the two UC subtypes identified previously. With a soft-thresholding power of $\beta = 17$, eight distinct modules were detected (Figure S1F). Correlation analysis with subtype features indicated that the brown module showed the strongest positive correlation with Cluster 1, comprising 216 genes (Figures 2B and S1G). By intersecting the gene sets from the pink and brown modules, 19 overlapping candidate signature genes were identified for further analysis (Figure 2C). To reduce dimensionality and eliminate redundancy, least absolute shrinkage and selection operator (LASSO) regression with tenfold cross-validation was employed, resulting in the selection of 10 genes (Figure 2D and E). Subsequently, a support vector machine (SVM) model was applied to the overlapping gene set for further screening, and the root mean square error (RMSE) reached its minimum when six genes were included (Figure 2F and G). Combining the results from both approaches, six potential core genes were identified: WARS1, Kynureninase (KYNU), Chitinase 3 Like 1 (CHI3L1), Plasminogen Activator, Urokinase (PLAU), Granzyme B (GZMB), and Caspase-4 (CASP4) (Figure 2H). To construct a predictive model for UC, 15 machine learning algorithms were utilized and evaluated using the merged dataset as well as three external validation cohorts (GSE47908, GSE48958, and GSE206171). The top 50 models, ranked by area under the curve (AUC), are presented in Figure 2I. Gene feature importance across the different models was calculated (Figure S2A), and a comprehensive integration of multiple models yielded the final ranking of predictive genes (Figure 2J).

Functional Analysis of Signature Genes in Active UC

Subsequent analyses were performed to validate the expression and diagnostic potential of the six identified signature genes. In independent test sets, all six genes—WARS1, KYNU, CHI3L1, PLAU, GZMB, and CASP4—were significantly upregulated in UC samples compared to healthy controls (Figure 3A), with AUC values exceeding 0.80, indicating

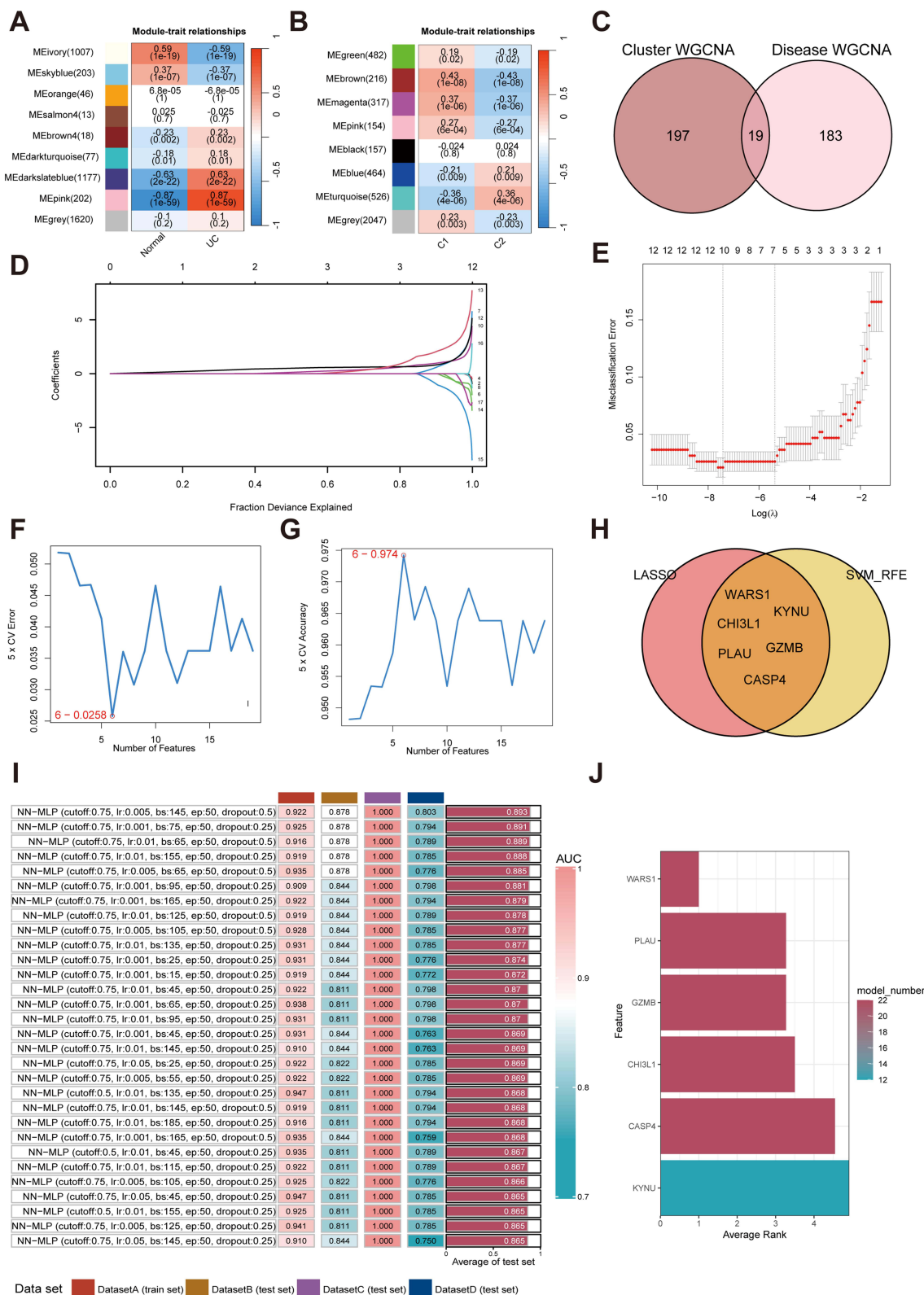


Figure 2 Verification of Signature Genes and Construction of a Prediction Model. **(A)** Heatmap displaying correlations between module eigengenes and UC status; red and blue indicate positive and negative correlations, respectively. **(B)** Correlation heatmap between module eigengenes and molecular subtypes. **(C)** Shared genes identified between disease-related and subtype-associated modules. **(D and E)** Feature selection using the LASSO regression model. **(F and G)** Key gene identification through SVM-RFE analysis. **(H)** Venn diagram showing common candidate genes identified by both machine learning approaches. **(I)** Integrated heatmap presenting the top 50 AUC values across datasets for each algorithm. **(J)** Bar plot ranking the importance scores of the six selected feature genes.

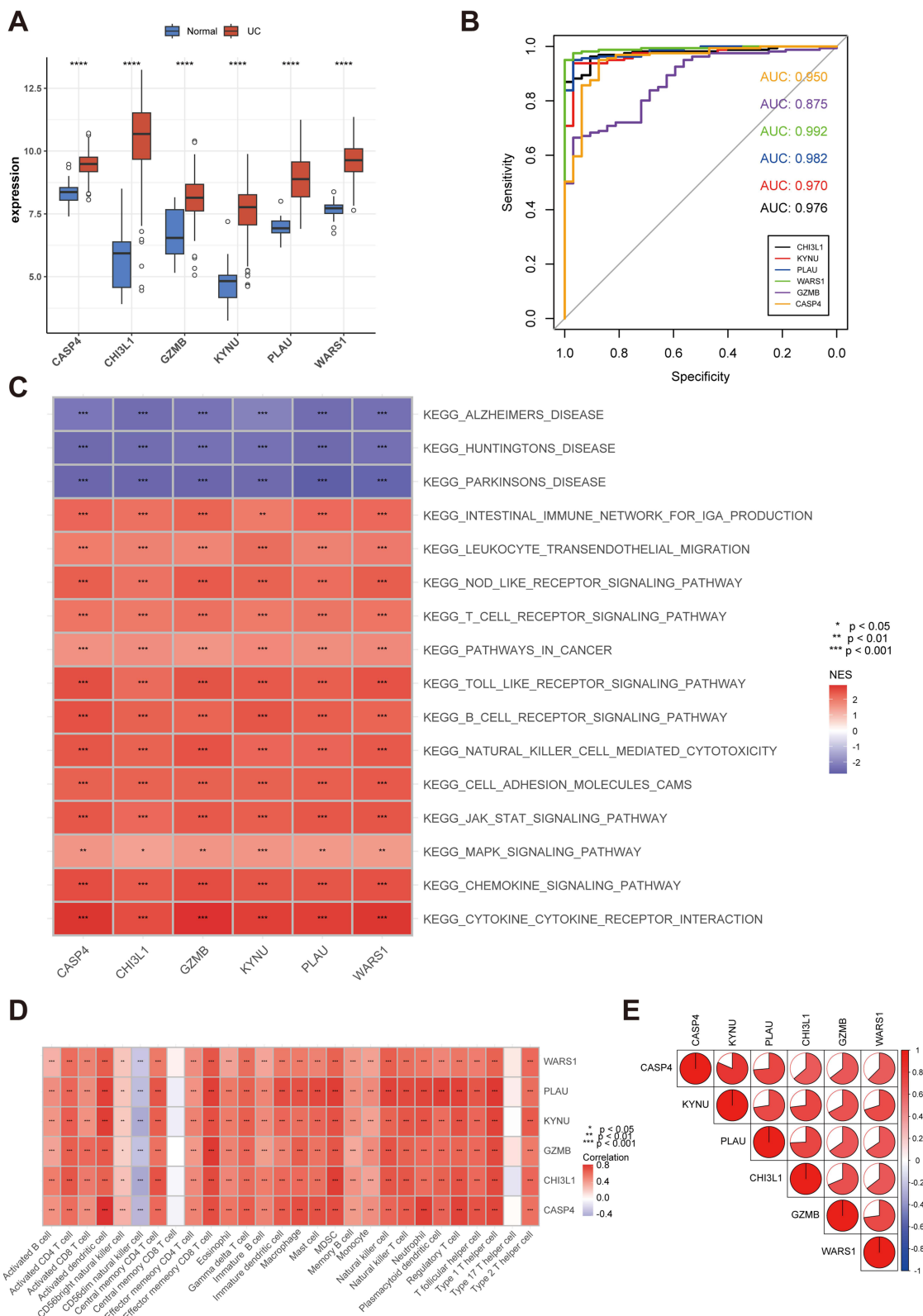


Figure 3 Functional Analysis of Signature Genes in Active UC. **(A)** Expression profiles of WARS1, KYNU, CHI3L1, PLAU, GZMB, and CASP4 in the training set. **(B)** ROC curves evaluating the diagnostic performance of signature genes in the training set. **(C)** GSEA results illustrating pathway enrichment of individual signature genes. **(D)** Correlation matrix showing associations between signature genes and 28 immune cell types. **(E)** Inter-gene correlation among the six signature genes. *P < 0.05, **P < 0.01, ***P < 0.001, ****P < 0.0001.

robust diagnostic performance (Figure 3B). Similarly, in the external validation set, the six genes remained significantly upregulated (Figure S2B), and their respective AUC values also demonstrated high diagnostic accuracy (Figure S2C). To elucidate the potential biological functions of these genes in active UC, Gene Set Enrichment Analysis (GSEA) was conducted. All six signature genes were positively enriched in multiple immune-related signaling pathways, including cytokine–cytokine receptor interaction, B cell receptor signaling, T cell receptor signaling, Toll-like receptor signaling, and the JAK-STAT pathway (Figure 3C). In contrast, these genes were negatively enriched in pathways associated with neurodegenerative disorders, such as Alzheimer’s disease, Huntington’s disease, and Parkinson’s disease (Figure 3C). Given the enrichment of immune-related pathways, we further investigated the association between the six signature genes and the infiltration of 28 immune cell types. A strong positive correlation was observed between the expression of these genes and various immune cell populations (Figure 3D), suggesting their involvement in immune activation. Furthermore, correlation analysis among the six signature genes revealed potential co-regulatory relationships (Figure 3E). Collectively, these results suggest that the signature genes may contribute to UC pathogenesis by modulating immune cell responses, potentially through synergistic mechanisms.

Single-Cell Transcriptomic Analysis of Selenoprotein-Related Genes in Ulcerative Colitis

Single-cell RNA sequencing analysis was performed on six UC tissue samples from the GSE214695 dataset using the Seurat R package. Through clustering and dimensionality reduction using principal component analysis (PCA) and uniform manifold approximation and projection (UMAP), 13 distinct cell types were identified and annotated: B cells, CD4⁺ T cells, CD8⁺ T cells, colonocytes, endothelial cells, fibroblasts, glial cells, goblet cells, macrophages, mast cells, neutrophils, plasma cells, and tuft cells (Figure 4A). Given that SELENOP is a key selenoprotein responsible for transporting approximately 60% of total serum selenium, further analysis focused on selenoproteins that were elevated in bulk transcriptome data, including SELENOP. The expression profiles of selenoprotein genes across the 13 identified cell types are shown in Figure 4B. Differential expression analysis between UC and healthy control samples was conducted using the FindMarkers function in Seurat. Results revealed significant upregulation of multiple selenoprotein genes in epithelial cell populations, particularly in colonocytes and goblet cells (Figure 4C).

In contrast, SELENOP expression was significantly downregulated in several immune cell populations, including macrophages, CD4⁺ T cells, CD8⁺ T cells, and neutrophils (Figure 4C). Given the critical role of macrophage polarization in modulating inflammatory responses in UC, we further explored the functional roles of key selenoproteins—specifically SELENOP, SELENOK, SELENOM, SELENOS, and GPX2—within macrophage populations. Based on the classification by Alba et al³⁰ we annotated macrophages into four distinct subtypes: M0 macrophages, M2 macrophages, inflammation-dependent alternative (IDA) macrophages, and M1 macrophages (Figure 4D). Recent studies suggest that resident macrophages typically fall into M0 or M2 subsets, whereas inflammatory macrophages are classified as either M1 or IDA types.³⁰ To better understand the transcriptional relationships among macrophage populations, we applied the unsupervised inference method Monocle 2 to construct potential transitional trajectories (Figures 4E and S3A) and generated faceted pseudotime plots illustrating the distribution of cells from each patient (Figure S3B). Previous studies have demonstrated that SELENOK plays a critical role in the migration of immune cells, including T cells, neutrophils, macrophages, and dendritic cells (DCs).^{33–36} By contrast, macrophages lacking SELENOP show markedly reduced migratory capacity.¹² Moreover, impaired SELENOP function correlates with enhanced M2 polarization.³⁷ Interestingly, SELENOP may suppress pro-inflammatory immune polarization, thereby mitigating inflammation-driven tumorigenesis.³⁸ This suggests a complex regulatory role in macrophage behavior and immune homeostasis. Additionally, SELENOS deficiency in macrophages promotes M1 polarization by targeting Ubiquitin A-52 Ribonucleoprotein (Uba52) to inhibit YAP ubiquitination and degradation.³⁹ In our analysis, the differentiation trajectory revealed notable changes in SELENOK and SELENOP expression (Figure 4F). After classifying macrophages into resident and inflammatory subtypes, we observed that inflammatory macrophages from UC patients significantly upregulated SELENOK and SELENOS, while downregulating SELENOP (Figure S3C). Collectively, these findings

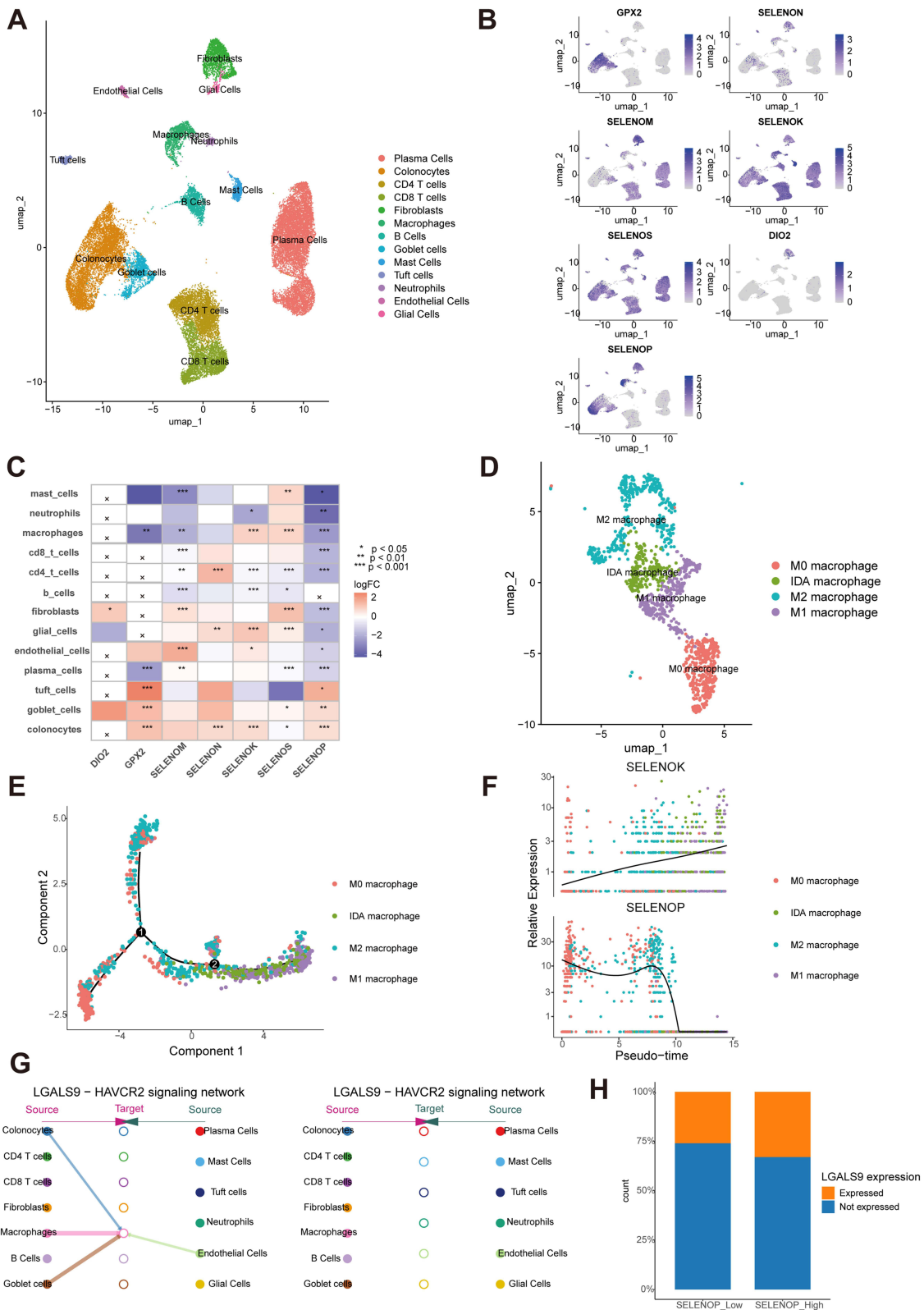


Figure 4 Single-Cell Transcriptomic Analysis of Selenoprotein-Related Genes in Ulcerative Colitis. **(A)** UMAP analysis showing identified cell types. **(B)** Feature plots showing selenoprotein genes expression in the 13 cell types. **(C)** Heat map showing the expression disparity of selenoprotein genes between UC and control groups. **(D)** UMAP of macrophage subtypes: M0, M2, IDA, and M1. **(E)** Monocle 2 pseudotime analysis reveals macrophage differentiation trajectories and transcriptional dynamics across subtypes. **(F)** Pseudotime-dependent expression of selenoproteins (SELENOP, SELENOK) across macrophage polarization states. **(G)** CellChat analysis reveals that intestinal epithelial cells regulate macrophage function through the LGALS9–HAVCR2 signaling axis. **(H)** Differential SELENOP expression in epithelial cells with varying LGALS9 expression levels. “x” denotes genes with no detectable expression in the corresponding cell type. Statistical significance is indicated as follows: ns, not significant; *P < 0.05; **P < 0.01; ***P < 0.001.

suggest that multiple selenoproteins cooperatively modulate macrophage polarization and function, playing pivotal roles in UC-associated inflammation and shaping the immune microenvironment.

To investigate the potential crosstalk between immune cells and epithelial cells, we conducted further analysis using CellChat. The results revealed that intestinal epithelial cells may regulate macrophage function through the LGALS9–HAVCR2 signaling axis (Figure 4G). Notably, epithelial cells with higher SELENOP expression also exhibited elevated LGALS9 levels, suggesting that the activity of this signaling pathway may be more pronounced in these cells (Figure 4H).

We applied the same algorithm to analyze the expression of signature genes at the single-cell level (Figure S3D–F). Among them, WARS1, CASP4, KYNU, and PLAU were broadly upregulated across most cell types. GZMB was mainly upregulated in immune cells, while CHI3L1 showed the highest expression in fibroblasts. Notably, inflammatory macrophages from UC patients displayed significant upregulation of WARS1, CASP4, and KYNU.

To further validate these results, we analyzed 12 additional samples from the GSE231993 dataset, which included UC and normal tissue samples from eight patients. After dimensionality reduction and clustering, we used the SingleR package to identify nine distinct cell types (Figure S4A). Subsequent refinement of monocyte clustering revealed four subsets: resident macrophages, infiltrating macrophages, DCs, and a minor proliferating macrophage population (Figure S4B). We then assessed expression differences and distribution patterns of selenoprotein genes and signature genes across these nine cell types (Figure S4C–F). Consistent with earlier findings, most selenoproteins were significantly upregulated in epithelial cells, while SELENOP showed marked downregulation in most non-epithelial cell types. Signature genes were also broadly elevated across nearly all cell types. Finally, differential analysis between resident and inflammatory macrophages yielded results similar to those previously described (Figure S4G). Further studies are required to elucidate the biological functions underlying these differences.

Validation of Differential Expression of Selenoproteins in Ulcerative Colitis

To investigate the differential expression of selenoprotein genes and six signature genes, we established a murine colitis model induced by DSS. After induction, we collected colonic tissues from both control and DSS-treated mice for molecular and histological analyses. Additionally, colonic tissue samples from five UC patients and five healthy individuals were obtained for further validation. qPCR revealed significant upregulation of several key selenoprotein genes, including DIO2, GPX2, SELENOM, SELENON, and SELENOS, in the DSS group compared to controls (Figure 5A). Among these, GPX2, SELENOM, and SELENON were further validated at the protein level by IHC (Figures 5B and S5A–B) and Western blotting (Figure 5C), both of which consistently confirmed their elevated expression in inflamed colonic tissues. Given the established roles of selenoproteins in maintaining redox homeostasis and mitigating oxidative stress, we next examined their inducibility under oxidative stress *in vitro*. Cells were treated with hydrogen peroxide (H₂O₂) to mimic oxidative damage, and gene expression dynamics were monitored over time. Notably, protein levels of GPX1/2, SELENOM, and SELENON increased in a time-dependent manner following H₂O₂ stimulation, suggesting their involvement in cellular antioxidant defense mechanisms (Figure 5D).

WARS1 as a Potential Therapeutic Target in Ulcerative Colitis

The analysis of signature genes validated the bioinformatic predictions, revealing significant upregulation in the DSS-treated group (Figure 6A). Given that WARS1 ranked highest in gene importance across multiple machine learning algorithms, we performed further investigation on this gene. Intracellularly, WARS1 primarily ligates tryptophan (Trp) to its corresponding tRNA for protein synthesis. Extracellularly, it also serves as an innate immune activator.⁴⁰ Previous studies have reported that IFN- γ -mediated secretion of WARS1 from mesenchymal stem cells (MSCs) contributes to the suppression of excessive inflammation and the progression of IBD,⁴¹ highlighting its immunomodulatory potential. Recent studies have shown that WARS1 downregulation affects cytosolic translation and mitochondrial protein synthesis, activating the mitochondrial unfolded protein response (UPRmt), which is an important pathway in cellular stress and inflammation.⁴² Overall, these findings suggest that WARS1 may play a significant role in UC.

To further explore the function of WARS1, we analyzed gene expression profiles from colonic mucosal samples of UC patients and healthy controls using four publicly available datasets (GSE75214, GSE13367, GSE38713, and

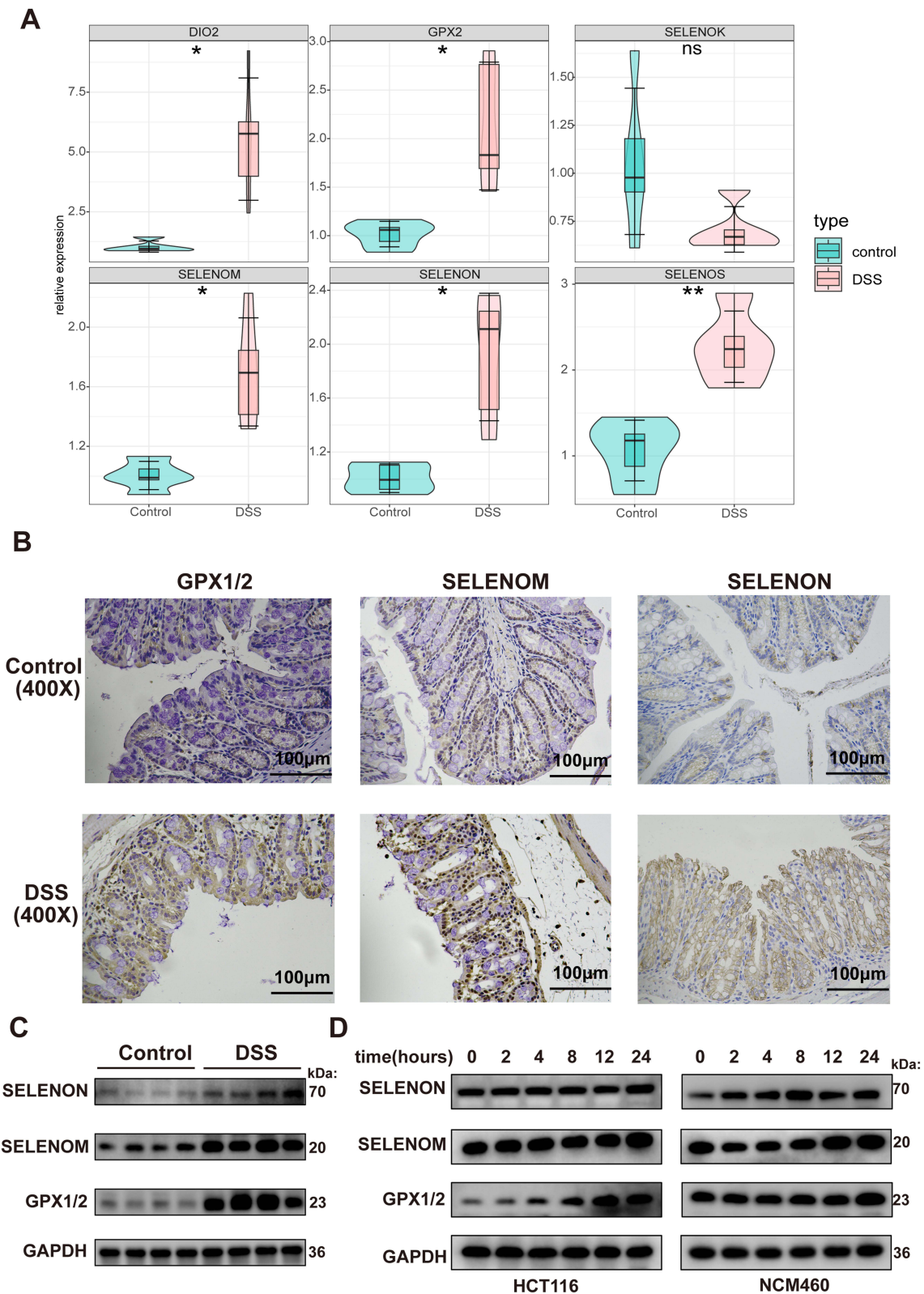


Figure 5 Validation of Differential Expression of Selenoproteins in Ulcerative Colitis. **(A)** The result of Real-time PCR analysis illustrated the expression levels of several key selenoprotein genes. **(B)** Immunohistochemistry experiment validating the expression of GPX1/2, SELENOM and SELENON in the colon of WT mice with UC. **(C)** GPX1/2, SELENOM and SELENON protein levels in the colon of WT mice with UC. **(D)** Western blot analysis of the dynamic expression of GPX1/2, SELENOM and SELENON in HCT116 cells and NCM460 cells during H₂O₂ (200µM) stimulation. Statistical significance is indicated as follows: ns, not significant; *P < 0.05; **P < 0.01.

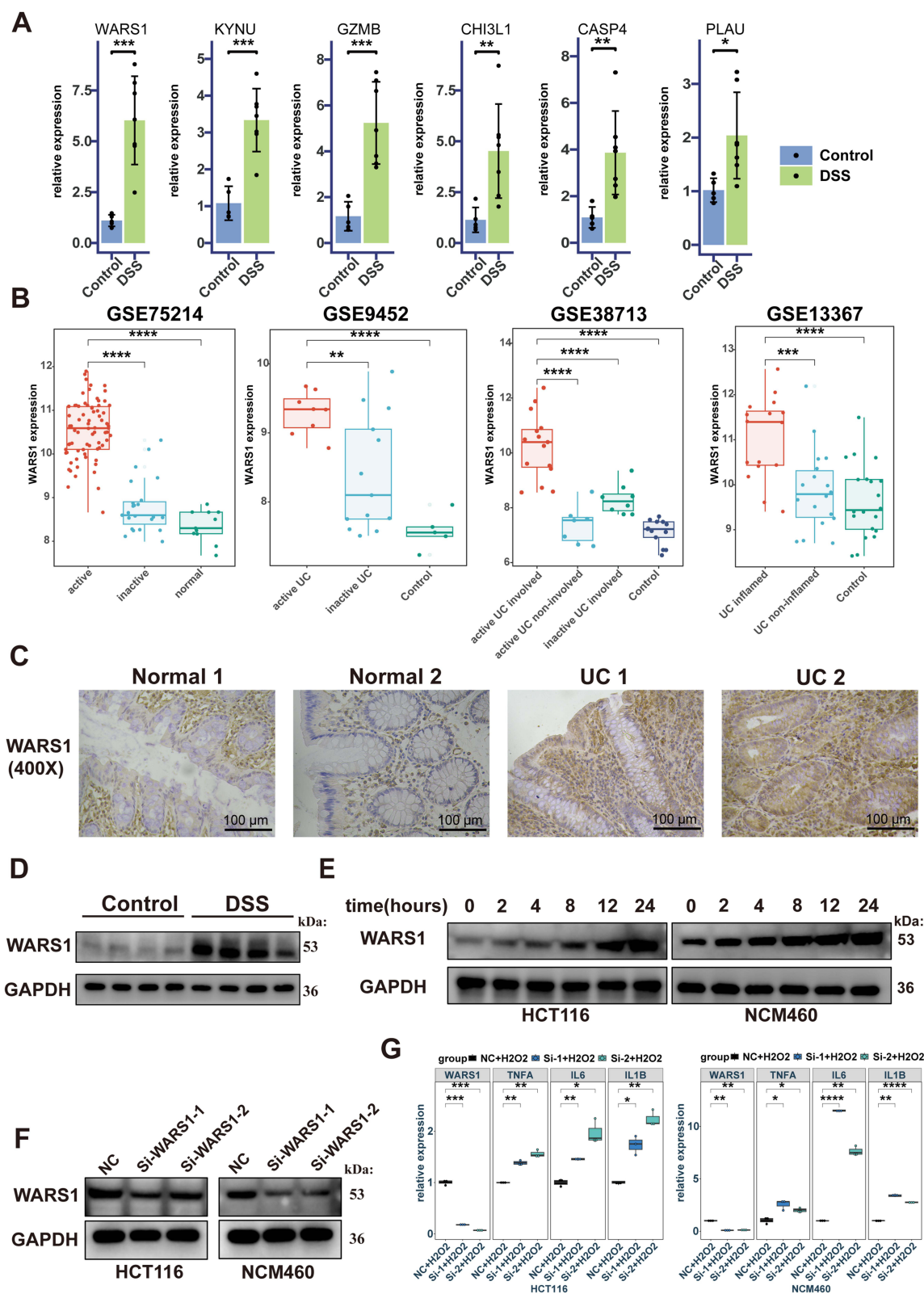


Figure 6 WARS1 as a Potential Therapeutic Target in Ulcerative Colitis. **(A)** The result of Real-time PCR analysis illustrated the expression levels of signature genes. **(B)** Expression levels of WARS1 mRNA in multiple GEO datasets. **(C)** Immunohistochemical staining images of WARS1 expression in inflamed intestinal tissues from UC patients and normal tissues from control subjects. **(D)** WARS1 protein levels in the colon of WT mice with UC. **(E)** Western blot analysis of dynamic expression of WARS1 in HCT116 and NCM460 cells during H_2O_2 ($200\mu M$) stimulation. **(F)** Western blot confirming WARS1 knockdown in HCT116 and NCM460 cells. **(G)** qPCR showing changes in inflammatory factors in WARS1 knockdown and control HCT116 and NCM460 cells. Statistical significance is indicated as follows: ns, not significant; * $P < 0.05$; ** $P < 0.01$; *** $P < 0.001$; **** $P < 0.0001$.

GSE9452) from the Gene Expression Omnibus (GEO). WARS1 expression was significantly higher in active UC patients compared to both healthy controls and those with inactive UC (Figure 6B). We further confirmed the elevated WARS1 protein levels in the DSS-treated group by immunohistochemistry (Figure 6C and S5C) and Western blotting (Figure 6D). Notably, WARS1 expression progressively increased in cells exposed to H₂O₂, suggesting a role in oxidative stress responses (Figure 6E). In addition, we observed a strong positive correlation between WARS1 and inflammatory cytokines including TNF- α , IL-1 β , and IL-6 in active UC patient samples (Figure S5D), implying its involvement in the inflammatory cascade. To validate this, we knocked down WARS1 in HCT116 and NCM460 cell lines (Figure 6F), which resulted in a marked upregulation of TNF- α , IL-1 β , and IL-6 (Figure 6G). Taken together, these findings indicate that WARS1 may function as a regulator of inflammation and oxidative stress in UC and could serve as a promising therapeutic target. However, further studies are needed to elucidate its precise role and underlying mechanisms.

Discussion

The incidence of UC has increased globally in recent years. Its pathogenesis involves genetic predisposition, epithelial barrier disruption, immune dysregulation, and environmental factors.² Current treatments aim to induce remission and improve quality of life, but often cause side effects and fail in some patients.^{43,44} Thus, novel therapies that resolve inflammation and promote intestinal healing are urgently needed.

Selenium and selenoproteins, due to their antioxidant and anti-inflammatory properties, are thought to protect against UC. The exacerbation of experimental colitis in selenium or selenoprotein deficiency highlights selenium's role in regulating inflammatory pathways and oxidative stress in the gut.¹⁰ Although several studies have reported on the roles of various selenoproteins in UC, a comprehensive analysis of the selenoprotein family in relation to UC remains lacking. Therefore, for the first time, we aimed to analyze the potential association of selenoproteins with UC from a bioinformatics perspective.

Intestinal barrier dysfunction and immune imbalance play central roles in UC onset and progression. Therefore, protecting intestinal epithelial cells and modulating immune and inflammatory responses represent two key therapeutic strategies. Our analysis indicates that the selenoprotein family may contribute to both processes. We identified six selenoproteins upregulated in active UC patients compared to controls. Single-cell data showed that most of these genes had significantly increased expression in epithelial cells. Conversely, SELENOP expression decreased markedly in most immune cells. SELENOP primarily functions as a selenium transporter and also acts as an extracellular antioxidant.⁴⁵ It is mainly produced by the liver and secreted into plasma, where it delivers selenium to tissues through its ten selenocysteine residues.⁴⁶ Within tissues, cells uptake and degrade SELENOP to release selenocysteines for the synthesis of other selenoproteins. Plasma SELENOP levels, together with selenium and GPx measurements, commonly assess selenium status.⁴⁷ Studies show that impaired SELENOP function promotes polarization toward M2 macrophages.³⁷ SELENOP deficiency compromises macrophage migration and disrupts intracellular selenoprotein balance.¹² The intestinal macrophage pool includes resident and infiltrating populations.⁴⁸ Resident macrophages generally suppress inflammation during UC,⁴⁹ whereas infiltrating monocytes differentiate into pro-inflammatory effectors.⁵⁰ Our results reveal a significant reduction of SELENOP in inflammatory macrophages relative to resident macrophages, possibly due to its consumption during immune activation. The broad decline of SELENOP across immune cells suggests it acts as a critical regulator during UC-associated immune responses.

Although we consistently observed SELENOP downregulation at the transcriptomic level in macrophages, its regulatory mechanism remains unclear. Whether this decrease results from transcriptional repression, defective uptake, or increased protein degradation requires further investigation. Future research using transcriptional reporter assays, mRNA stability studies, and protein turnover experiments will clarify how SELENOP expression is controlled in macrophages and how this regulation affects intestinal immune homeostasis. Moreover, this study offers preliminary evidence of immune–epithelial crosstalk via the LGALS9–HAVCR2 signaling axis, especially in epithelial cells expressing high levels of SELENOP. While these findings provide novel mechanistic insights, additional functional experiments are necessary to confirm the biological significance of this pathway and elucidate the role of selenoproteins in intercellular communication during UC.

In this study, WARS1, CHI3L1, GZMB, KYNU, PLAU, and CASP4 were identified as critical biomarkers for the diagnosis of UC. Previous studies reported downregulation of WARS1 in a DSS-induced experimental colitis model.⁵¹ Furthermore, it has been demonstrated that WARS1 inhibits the proliferation of CD4+ T cells derived from hUCB-MSCs by promoting apoptosis.⁵¹ However, recent research suggests that secreted WARS1, an endogenous ligand for Toll-like receptor (TLR) 2 and TLR4 involved in infection response, is a key activator of genes characteristic of a hyperinflammatory sepsis phenotype.⁵² Our study shows that WARS1 is significantly upregulated in active UC and gradually increases with prolonged oxidative stress. Knockdown of WARS1 leads to an increase in the expression of inflammatory factors, suggesting that it is more likely to act as a regulator in response to inflammation and oxidative stress. CHI3L1, a glycoprotein implicated in various diseases, including IBD, exerts its influence on multiple components of both the innate and adaptive immune responses.⁵³ GZMB, a serine protease extensively studied for its role in cytotoxic lymphocyte-mediated apoptosis, has been identified as a promising biomarker for detecting active IBD and predicting treatment response.⁵⁴ KYNU is a hydrolase involved in tryptophan metabolism. The silencing of KYNU has been shown to suppress inflammatory responses in intestinal epithelial cells under IL-1 β stimulation.⁵⁵ PLAU encodes the urokinase-type plasminogen activator (uPA), which converts plasminogen to plasmin, a potent protease involved in fibrinolysis and extracellular matrix (ECM) degradation. A recent study suggests that local nutrient deprivation may serve as a candidate mechanism for PLAU upregulation in intestinal fibroblasts, a process that could be further amplified by IBD risk factors.⁵⁶ The CASP4 gene encodes a protein that plays a role in immunity and inflammatory processes.⁵⁷ Human caspases-4 and -5 have been shown to be elevated in the stromal tissue of patients with UC, and their expression levels are correlated with disease activity and inflammation scores.⁵⁸ In conclusion, the six signature genes identified in this study are closely linked to the pathogenesis of UC and could be potential targets for early diagnosis and treatment of the disease.

To summarize, our study highlights the potential contribution of SeMet-related genes and selenoproteins to UC pathogenesis, proposing new molecular targets for intervention. Nevertheless, our findings are primarily based on bioinformatics and *in vitro* analyses, with limited *in vivo* validation. Importantly, our *in vivo* data are restricted to the DSS-induced colitis model, which—despite its reproducibility—mainly reflects epithelial injury and innate immune responses. Given the multifactorial nature of UC and the involvement of adaptive immunity, future studies should incorporate complementary models, such as the T cell transfer colitis model, to validate the universality of selenoprotein alterations and further elucidate their immunoregulatory roles.

Conclusion

In summary, this study identified 11 SeMet-related genes that were significantly upregulated in UC patients, revealing their association with immune cells. Additionally, six signature genes (WARS1, KYNU, GZMB, CHI3L1, PLAU, and CASP4) were identified, and based on these genes, a highly accurate predictive model was developed. Among these, WARS1 was notably upregulated in response to oxidative stress, and its knockdown resulted in elevated levels of inflammatory cytokines, underscoring its critical role in the pathogenesis of UC. Single-cell RNA sequencing demonstrated that selenoproteins were predominantly expressed in epithelial cells and may protect epithelial cells from oxidative stress. These findings provide new insights into the early diagnosis and potential therapeutic targets for UC.

Abbreviations

AUC, Area Under the Curve; CASP4, Caspase-4; CDF, Cumulative Distribution Function; CHI3L1, Chitinase 3 Like 1; DCs, Dendritic Cells; DIO, Iodothyronine Deiodinases; DRGs, Differentially Regulated Genes; DSS, Dextran Sulfate Sodium; ECM, Extracellular Matrix; EGFR, Epidermal Growth Factor Receptor; ER, Endoplasmic Reticulum; GPx, Glutathione Peroxidases; GSEA, Gene Set Enrichment Analysis; GSEA, Gene Set Variation Analysis; GZMB, Granzyme B; H₂O₂, Hydrogen Peroxide; IBD, Inflammatory Bowel Disease; IDA, Inflammation-Dependent Alternative; IHC, Immunohistochemistry; LASSO, Least Absolute Shrinkage and Selection Operator; MSCs, Mesenchymal Stem Cells; MSigDB, Molecular Signatures Database; PCA, Principal Component Analysis; PLAU, Plasminogen Activator, Urokinase; qPCR, Quantitative Polymerase Chain Reaction; RMSE, Root Mean Square Error; scRNA-seq, Single-Cell RNA Sequencing; Se, Selenium; Sec, Selenocysteine; SeMet, Selenium metabolism and selenoproteins; ssGSEA, Single-

Sample Gene Set Enrichment Analysis; SVM, Support Vector Machine; TLR, Toll-like Receptor; Trp, Tryptophan; TrxR, Thioredoxin Reductases; Uba52, Ubiquitin A-52 Ribonucleoprotein; UC, Ulcerative Colitis; UMAP, Uniform Manifold Approximation and Projection; UPRmt, Mitochondrial Unfolded Protein Response; uPA, Urokinase-type Plasminogen Activator; WARS1, Tryptophanyl-tRNA Synthetase 1; WGCNA, Weighted Gene Co-expression Network Analysis; YAP1, Yes-associated Protein 1.

Author Contributions

All authors made a significant contribution to the work reported, whether that is in the conception, study design, execution, acquisition of data, analysis and interpretation, or in all these areas; took part in drafting, revising or critically reviewing the article; gave final approval of the version to be published; have agreed on the journal to which the article has been submitted; and agree to be accountable for all aspects of the work.

Funding

The work was supported by the Zhejiang Provincial Natural Science Foundation (LHDMZ23H160003).

Disclosure

The authors declare that they have no competing interests.

References

- Vegh Z, Kurti Z, Lakatos PL. Epidemiology of inflammatory bowel diseases from west to east. *J Dig Dis*. 2017;18(2):92–98. doi:10.1111/1751-2980.12449
- Ungaro R, Mehandru S, Allen PB, Peyrin-Biroulet L, Colombel JF. Ulcerative colitis. *Lancet*. 2017;389(10080):1756–1770. doi:10.1016/S0140-6736(16)32126-2
- Papp LV, Lu J, Holmgren A, Khanna KK. From selenium to selenoproteins: synthesis, identity, and their role in human health. *Antioxid Redox Signal*. 2007;9(7):775–806. doi:10.1089/ars.2007.1528
- Barrett CW, Singh K, Motley AK, et al. Dietary selenium deficiency exacerbates DSS-induced epithelial injury and AOM/DSS-induced tumorigenesis. *PLoS One*. 2013;8(7):e67845. doi:10.1371/journal.pone.0067845
- Krehl S, Loewinger M, Florian S, et al. Glutathione peroxidase-2 and selenium decreased inflammation and tumors in a mouse model of inflammation-associated carcinogenesis whereas sulforaphane effects differed with selenium supply. *Carcinogenesis*. 2012;33(3):620–628. doi:10.1093/carcin/bgr288
- Labunskyy VM, Hatfield DL, Gladyshev VN. Selenoproteins: molecular pathways and physiological roles. *Physiol Rev*. 2014;94(3):739–777. doi:10.1152/physrev.00039.2013
- Gladyshev VN, Arner ES, Berry MJ, et al. Selenoprotein gene nomenclature. *J Biol Chem*. 2016;291(46):24036–24040. doi:10.1074/jbc.M116.756155
- Tinggi U. Selenium: its role as antioxidant in human health. *Environ Health Prev Med*. 2008;13(2):102–108. doi:10.1007/s12199-007-0019-4
- Esworthy RS, Aranda R, Martin MG, Doroshov JH, Binder SW, Chu FF. Mice with combined disruption of Gpx1 and Gpx2 genes have colitis. *Am J Physiol Gastrointest Liver Physiol*. 2001;281(3):G848–855. doi:10.1152/ajpgi.2001.281.3.G848
- Speckmann B, Steinbrenner H. Selenium and selenoproteins in inflammatory bowel diseases and experimental colitis. *Inflamm Bowel Dis*. 2014;20(6):1110–1119. doi:10.1097/MIB.0000000000000020
- Speckmann B, Gerloff K, Simms L, et al. Selenoprotein S is a marker but not a regulator of endoplasmic reticulum stress in intestinal epithelial cells. *Free Radic Biol Med*. 2014;67:265–277. doi:10.1016/j.freeradbiomed.2013.11.001
- Short SP, Pilat JM, Barrett CW, et al. Colonic epithelial-derived selenoprotein P is the source for antioxidant-mediated protection in colitis-associated cancer. *Gastroenterology*. 2021;160(5):1694–1708e1693. doi:10.1053/j.gastro.2020.12.059
- Huang X, Yang X, Zhang M, et al. SELENOI functions as a key modulator of ferroptosis pathway in colitis and colorectal cancer. *Adv Sci*. 2024;11(28):e2404073. doi:10.1002/advs.202404073
- Nettleford SK, Liao C, Short SP, Rossi RM, Singh V, Prabhu KS. Selenoprotein W ameliorates experimental colitis and promotes intestinal epithelial repair. *Antioxidants*. 2023;12(4). doi:10.3390/antiox12040850
- Vancamelbeke M, Vanuytsel T, Farre R, et al. Genetic and transcriptomic bases of intestinal epithelial barrier dysfunction in inflammatory bowel disease. *Inflamm Bowel Dis*. 2017;23(10):1718–1729. doi:10.1097/MIB.0000000000001246
- Li K, Strauss R, Ouahed J, et al. Molecular comparison of adult and pediatric ulcerative colitis indicates broad similarity of molecular pathways in disease tissue. *J Pediatr Gastroenterol Nutr*. 2018;67(1):45–52. doi:10.1097/MPG.0000000000001898
- Bjerrum JT, Nielsen OH, Riis LB, et al. Transcriptional analysis of left-sided colitis, pancolitis, and ulcerative colitis-associated dysplasia. *Inflamm Bowel Dis*. 2014;20(12):2340–2352. doi:10.1097/MIB.0000000000000235
- Van der Goten J, Vanhove W, Lemaire K, et al. Integrated miRNA and mRNA expression profiling in inflamed colon of patients with ulcerative colitis. *PLoS One*. 2014;9(12):e116117. doi:10.1371/journal.pone.0116117
- Olsen J, Gerds TA, Seidelin JB, et al. Diagnosis of ulcerative colitis before onset of inflammation by multivariate modeling of genome-wide gene expression data. *Inflamm Bowel Dis*. 2009;15(7):1032–1038. doi:10.1002/ibd.20879

20. Planell N, Lozano JJ, Mora-Buch R, et al. Transcriptional analysis of the intestinal mucosa of patients with ulcerative colitis in remission reveals lasting epithelial cell alterations. *Gut*. 2013;62(7):967–976. doi:10.1136/gutjnl-2012-303333
21. Bjerrum JT, Hansen M, Olsen J, Nielsen OH. Genome-wide gene expression analysis of mucosal colonic biopsies and isolated colonocytes suggests a continuous inflammatory state in the lamina propria of patients with quiescent ulcerative colitis. *Inflamm Bowel Dis*. 2010;16(6):999–1007. doi:10.1002/ibd.21142
22. Barbie DA, Tamayo P, Boehm JS, et al. Systematic RNA interference reveals that oncogenic KRAS-driven cancers require TBK1. *Nature*. 2009;462(7269):108–112. doi:10.1038/nature08460
23. Charoentong P, Finotello F, Angelova M, et al. Pan-cancer immunogenomic analyses reveal genotype-immunophenotype relationships and predictors of response to checkpoint blockade. *Cell Rep*. 2017;18(1):248–262. doi:10.1016/j.celrep.2016.12.019
24. Wilkerson MD, Hayes DN. ConsensusClusterPlus: a class discovery tool with confidence assessments and item tracking. *Bioinformatics*. 2010;26(12):1572–1573. doi:10.1093/bioinformatics/btq170
25. Langfelder P, Horvath S. WGCNA: an R package for weighted correlation network analysis. *BMC Bioinf*. 2008;9(1):559. doi:10.1186/1471-2105-9-559
26. Sharma R, Bhullar A, Bansal P, Kaur G, Gupta VJM. Bioinformatics analysis identifies potential hub genes, therapeutic agents, and crucial pathways in the pathogenesis of refeeding disease. *Medinformatics*. 2023. doi:10.47852/bonviewMEDIN32021516
27. Alhatemi RAJ, Savaş SJM, van Veldhoven RPJ, Verhagen E, Fiore A. A weighted ensemble approach with multiple pre-trained deep learning models for classification of stroke. *Npj Nanophotonics*. 2024;1(1):10–19. doi:10.1038/s44310-024-00011-y
28. Charles S, Natarajan JJM. Identification of key gene modules and novel transcription factors in tetralogy of fallot using machine learning and network topological features. *Medinformatics*. 2024;1(1):27–34.
29. Yu G, Wang LG, Han Y, He QY. clusterProfiler: an R package for comparing biological themes among gene clusters. *OMICS*. 2012;16(5):284–287. doi:10.1089/omi.2011.0118
30. Garrido-Trigo A, Corraliza AM, Veny M, et al. Macrophage and neutrophil heterogeneity at single-cell spatial resolution in human inflammatory bowel disease. *Nat Commun*. 2023;14(1):4506. doi:10.1038/s41467-023-40156-6
31. Du J, Zhang J, Wang L, et al. Selective oxidative protection leads to tissue topological changes orchestrated by macrophage during ulcerative colitis. *Nat Commun*. 2023;14(1):3675. doi:10.1038/s41467-023-39173-2
32. Carlson BA, Moustafa ME, Sengupta A, et al. Selective restoration of the selenoprotein population in a mouse hepatocyte selenoproteinless background with different mutant selenocysteine tRNAs lacking Um34. *J Biological Chem*. 2007;282(45):32591–32602. doi:10.1074/jbc.M707036200
33. Huang Z, Hoffmann FW, Norton RL, Hashimoto AC, Hoffmann PR. Selenoprotein K is a novel target of m-calpain, and cleavage is regulated by toll-like receptor-induced calpastatin in macrophages. *J Biol Chem*. 2011;286(40):34830–34838. doi:10.1074/jbc.M111.265520
34. Meng XL, Chen CL, Liu YY, et al. Selenoprotein SELENOK enhances the migration and phagocytosis of microglial cells by increasing the cytosolic free Ca²⁺ level resulted from the up-regulation of IP(3)R. *Neuroscience*. 2019;406:38–49. doi:10.1016/j.neuroscience.2019.02.029
35. Norton RL, Fredericks GJ, Huang Z, Fay JD, Hoffmann FW, Hoffmann PR. Selenoprotein K regulation of palmitoylation and calpain cleavage of ASAP2 is required for efficient FcγR-mediated phagocytosis. *J Leukoc Biol*. 2017;101(2):439–448. doi:10.1189/jlb.2A0316-156RR
36. Verma S, Hoffmann FW, Kumar M, et al. Selenoprotein K knockout mice exhibit deficient calcium flux in immune cells and impaired immune responses. *J Immunol*. 2011;186(4):2127–2137. doi:10.4049/jimmunol.1002878
37. Barrett CW, Reddy VK, Short SP, et al. Selenoprotein P influences colitis-induced tumorigenesis by mediating stemness and oxidative damage. *J Clin Investigat*. 2015;125(7):2646–2660. doi:10.1172/JCI76099
38. Barrett CW, Short SP, Williams CS, Williams CSJC, sciences mL. Selenoproteins and oxidative stress-induced inflammatory tumorigenesis in the gut. *Cell Mol Life Sci*. 2017;74(4):607–616. doi:10.1007/s00018-016-2339-2
39. Yao Y, Xu T, Li X, et al. Selenoprotein S maintains intestinal homeostasis in ulcerative colitis by inhibiting necroptosis of colonic epithelial cells through modulation of macrophage polarization. *Theranostics*. 2024;14(15):5903–5925. doi:10.7150/thno.97005
40. Ahn YH, Park S, Choi JJ, et al. Corrigendum: secreted tryptophanyl-tRNA synthetase as a primary defence system against infection. *Nature Microbiol*. 2017;2(3):17015. doi:10.1038/nmicrobiol.2017.15
41. Kang I, Lee B-C, Lee JY, et al. Interferon-γ-mediated secretion of tryptophanyl-tRNA synthetases has a role in protection of human umbilical cord blood-derived mesenchymal stem cells against experimental colitis. *BMB Reports*. 2019;52(5):318. doi:10.5483/BMBRep.2019.52.5.134
42. Pontanari F, Demagny H, Faure A, et al. Wars1 downregulation in hepatocytes induces mitochondrial stress and disrupts metabolic homeostasis. *Metabolism*. 2025;162:156061. doi:10.1016/j.metabol.2024.156061
43. Turner D, Ricciuto A, Lewis A, et al. STRIDE-II: an update on the selecting therapeutic targets in inflammatory bowel disease (STRIDE) initiative of the international organization for the study of IBD (IOIBD): determining therapeutic goals for treat-to-target strategies in IBD. *Gastroenterology*. 2021;160(5):1570–1583. doi:10.1053/j.gastro.2020.12.031
44. Vulliamoz M, Brand S, Juillerat P, et al. TNF-alpha blockers in inflammatory bowel diseases: practical recommendations and a user's guide: an update. *Digestion*. 2020;101 Suppl 1(Suppl. 1):16–26. doi:10.1159/000506898
45. Burk RF, Hill KE. Selenoprotein P-expression, functions, and roles in mammals. *Biochim Biophys Acta*. 2009;1790(11):1441–1447. doi:10.1016/j.bbagen.2009.03.026
46. Burk RF, Hill KE. Selenoprotein P: an extracellular protein with unique physical characteristics and a role in selenium homeostasis. *Annu Rev Nutr*. 2005;25(1):215–235. doi:10.1146/annurev.nutr.24.012003.132120
47. Short SP, Pilat JM, Williams CS. Roles for selenium and selenoprotein P in the development, progression, and prevention of intestinal disease. *Free Radic Biol Med*. 2018;127:26–35. doi:10.1016/j.freeradbiomed.2018.05.066
48. Sheng J, Ruedl C, Karjalainen K. Most tissue-resident macrophages except microglia are derived from fetal hematopoietic stem cells. *Immunity*. 2015;43(2):382–393. doi:10.1016/j.immuni.2015.07.016
49. Zigmund E, Bernshtein B, Friedlander G, et al. Macrophage-restricted interleukin-10 receptor deficiency, but not IL-10 deficiency, causes severe spontaneous colitis. *Immunity*. 2014;40(5):720–733. doi:10.1016/j.immuni.2014.03.012
50. Zigmund E, Varol C, Farache J, et al. Ly6C hi monocytes in the inflamed colon give rise to proinflammatory effector cells and migratory antigen-presenting cells. *Immunity*. 2012;37(6):1076–1090. doi:10.1016/j.immuni.2012.08.026

51. Kang I, Lee BC, Lee JY, et al. Interferon-gamma-mediated secretion of tryptophanyl-tRNA synthetases has a role in protection of human umbilical cord blood-derived mesenchymal stem cells against experimental colitis. *BMB Rep.* 2019;52(5):318–323.
52. Kim YT, Huh JW, Choi YH, et al. Highly secreted tryptophanyl tRNA synthetase 1 as a potential theranostic target for hypercytokinemic severe sepsis. *EMBO Mol Med.* 2024;16(1):40–63. doi:10.1038/s44321-023-00004-y
53. Deutschmann C, Roggenbuck D, Schierack P. The loss of tolerance to CHI3L1 - A putative role in inflammatory bowel disease? *Clin Immunol.* 2019;199:12–17. doi:10.1016/j.clim.2018.12.005
54. Heidari P, Haj-Mirzaian A, Prabhu S, Ataenia B, Esfahani SA, Mahmood U. Granzyme B PET imaging for assessment of disease activity in inflammatory bowel disease. *J Nucl Med.* 2024;65(7):1137–1143. doi:10.2967/jnumed.123.267344
55. Shi Y, Luo S, Zhai J, Chen Y. A novel causative role of imbalanced kynurenine pathway in ulcerative colitis: upregulation of KMO and KYNU promotes intestinal inflammation. *Biochim Biophys Acta Mol Basis Dis.* 2024;1870(2):166929. doi:10.1016/j.bbadis.2023.166929
56. Secchia S, Beilinson V, Chen X, et al. Nutrient starvation activates ECM remodeling gene enhancers associated with inflammatory bowel disease risk in fibroblasts. *BioRxiv.* 2024. doi:10.1101/2024.09.06.611754
57. McIlwain DR, Berger T, Mak TW. Caspase functions in cell death and disease. *Cold Spring Harb Perspect Biol.* 2015;7(4):a026716. doi:10.1101/cshperspect.a026716
58. Flood B, Oficjalska K, Laukens D, et al. Altered expression of caspases-4 and -5 during inflammatory bowel disease and colorectal cancer: diagnostic and therapeutic potential. *Clin Exp Immunol.* 2015;181(1):39–50. doi:10.1111/cei.12617

Journal of Inflammation Research

Publish your work in this journal

The Journal of Inflammation Research is an international, peer-reviewed open-access journal that welcomes laboratory and clinical findings on the molecular basis, cell biology and pharmacology of inflammation including original research, reviews, symposium reports, hypothesis formation and commentaries on: acute/chronic inflammation; mediators of inflammation; cellular processes; molecular mechanisms; pharmacology and novel anti-inflammatory drugs; clinical conditions involving inflammation. The manuscript management system is completely online and includes a very quick and fair peer-review system. Visit <http://www.dovepress.com/testimonials.php> to read real quotes from published authors.

Submit your manuscript here: <https://www.dovepress.com/journal-of-inflammation-research-journal>

Dovepress

Taylor & Francis Group